

Supplementary Information

**Energy-dense anode-free rechargeable lithium metal
batteries based on thick cathodes and pulse charging
strategies**

Experimental section

Materials

1,3-Dioxlane (DOL, >99.8%) and lithium nitrate (LiNO_3 , >99.99%) were purchased from Sigma-Aldrich. 1,2-diethoxyethane (DEE, 98.0%) were purchased from TCI. Lithium bis(fluorosulfonyl)imide (LiFSI, >99.99%) was purchased from DoDoChem. LFP powder, conductive carbon black (Super P) and PVDF were provided from Tianjin EV Energies Co., Ltd (JEVE). NCM811 powder were purchased from Guangdong Candlelight New Energy Technology Co. Ltd. Carbon paper and 50 μm Li foil were purchased from Tianjin Eilian Electronic Technology Co., Ltd. All materials are used without further treatment.

Electrode preparation and cell assembly

CR2032 coin cells were assembled in a glove box filled with Ar (MIKROUNA, $\text{H}_2\text{O} < 0.1$ ppm, $\text{O}_2 < 0.1$ ppm) for electrochemical measurement. For the preparation of LFP cathode with areal capacity of 0.5 mAh/cm^2 , LFP, PVDF, and super P with a weight ratio of 8:1:1 was mixed in N-methyl pyrrolidone (NMP) solvent (Aladdin) to form the uniform slurry, which was then evenly scraped onto the 16 μm Al current collector. The slurry was then dried at 100 $^\circ\text{C}$ in a vacuum oven to finally obtain the 0.5LFP cathode. LFP cathodes with areal capacity of 2.5 mAh/cm^2 and 5 mAh/cm^2 (Electrode density: 2.50 g/cm^3 , active material ratio: 97.40%, nominal specific capacity: 150 mAh/g) were provided from Tianjin EV Energies Co., Ltd (JEVE). For the preparation of thin NCM811 cathode, NCM811 powder, PVDF, and super P with a weight ratio of 8:1:1 was mixed in N-methyl pyrrolidone (NMP) solvent (Aladdin) to form the uniform slurry, the remaining operations are consistent with LFP. Thick NCM811 cathode was kindly provided by Golden Feather New Energy Co., Ltd. The diameter of all cathodes was 10 mm. For the full cells assembled by LFP cathode (diameter of 10 mm), 2 M LiFSI in DOL with 0.5 M LiNO_3 was used as the electrolyte (60 μL). For the full cells assembled by NCM811 cathode, 4 M LiFSI in DEE was used as the electrolyte (60 μL). The Al_2O_3 coated celgard film with a diameter of 19 mm was used as the separator. For LMBs, Li foil with a diameter of 16 mm was used as anode. For AFLMBs, Cu foil with a diameter of 16 mm was used as the anode current collector.

Materials Characterizations and electrochemical tests

Scanning electron microscopy (SEM, JEOL JSM7500F) were used to investigate the morphology of Li deposition. Galvanostatic charge-discharge tests of all batteries were conducted on LAND battery test system (Land CT3002A) at room temperature. If there is no special explanation, a formation cycle was conducted for all the batteries at a current density of 0.25 mA/cm². For the full cells assembled by LFP cathode, all the batteries were operated between 3.0 and 3.8 V. For the full cells assembled by NCM811 cathode, all the batteries were operated between 3.0 and 4.3 V. For pc2,1 pulsed charge strategy, the batteries were periodically charged at 0.75 mA/cm² for 2s and rested for 1s until the voltage reached 3.8V (LFP cathode) or 4.3V (NCM811 cathode). For pc1,1 pulsed charge strategy, the batteries were periodically charged at 1 mA/cm² for 1s and rested for 1s. The electrochemical impedance spectroscopy (EIS) was conducted on the Electrochemical workstation (CHI 760E) in the frequency range 0.1 Hz–10⁵ Hz with an amplitude of 5 mV at room temperature. A series of Cu||5LFP anode-free full cells were firstly cycled by conventional charge process at a current density of 0.5 mA/cm². The similar resistance at the formation cycle confirms the accuracy of characterizations. Then in the following cycles, the EIS at high current density either by conventional charge process (5 mA/cm²) or pulsed charge process (periodically charged for 1s at 10 mA/cm² and rested for 1s) were measured.

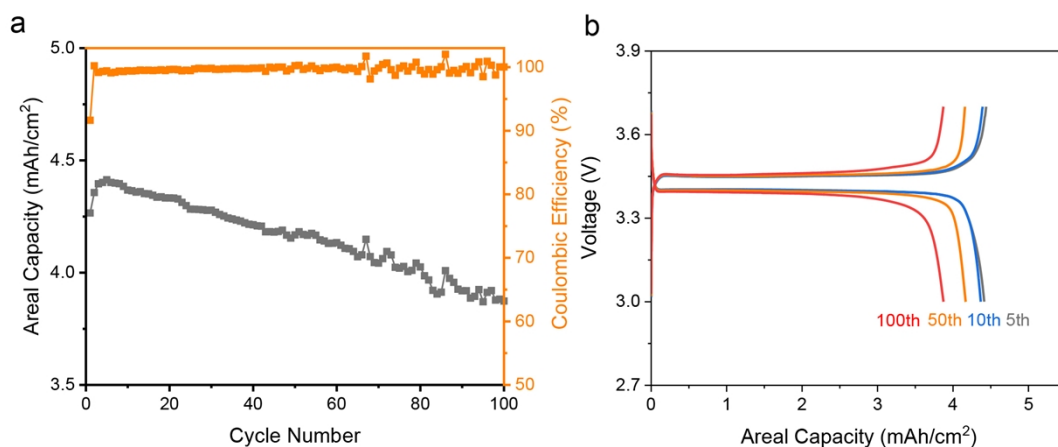


Figure S1 Electrochemical performance of Li||5LFP. a, Cycling performance with CEs of Li||5LFP batteries. **b,** The corresponding galvanostatic charge/discharge profiles of Li||5LFP. The batteries were first cycled at a current density of 0.25 mA/cm² for the formation cycle, followed by charge/discharge a current density of 0.5 mA/cm² and a voltage range of 3.0 and 3.8 V.

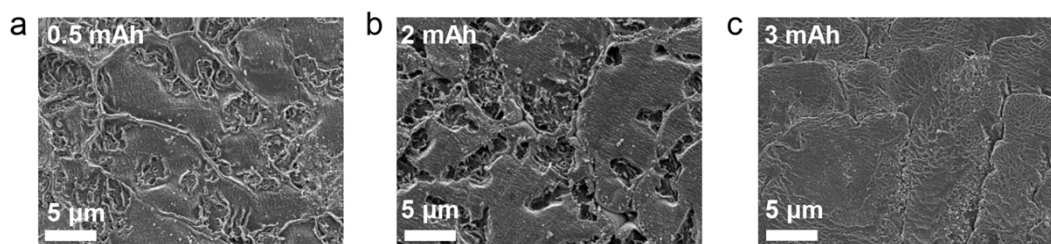


Figure S2 SEM Morphology characterization of deposited Li in Cu||5LFP batteries at different deposition capacities. a, 0.5 mAh, b, 2 mAh, c, 3 mAh.

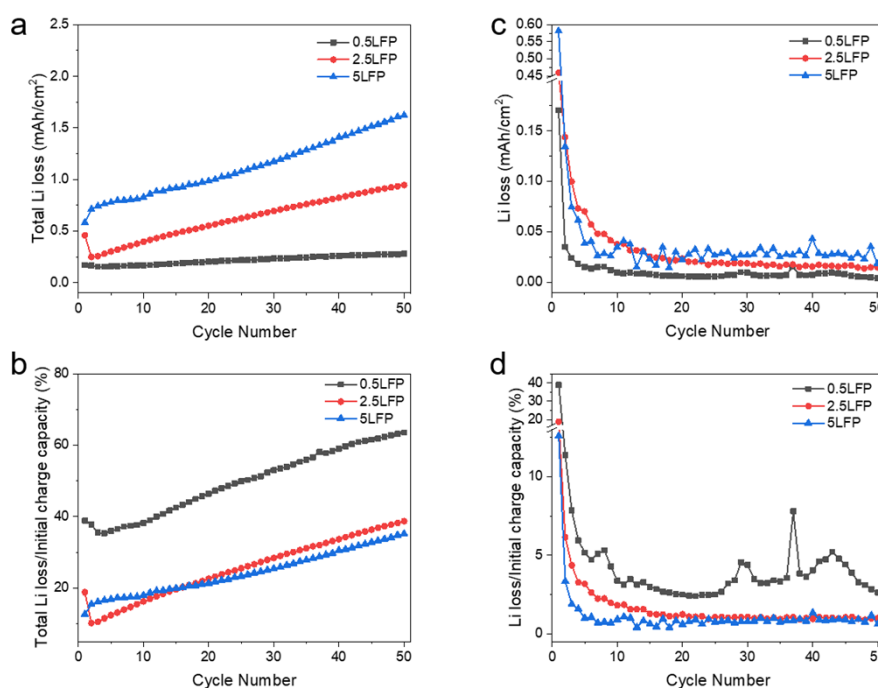


Figure S3 Quantification of Li losses in Cu||LFP AFLMBs. a, The total Li loss relative to the initial charging capacity and **b,** corresponding percentage to the initial charge capacity. **c,** The Li loss of each cycle relative to the previous cycle and **d,** corresponding percentage to the initial charge capacity. (Total Li loss = 1st charge capacity – nth discharge capacity, Li loss of per cycle = (nth charge capacity – nth discharge capacity)).

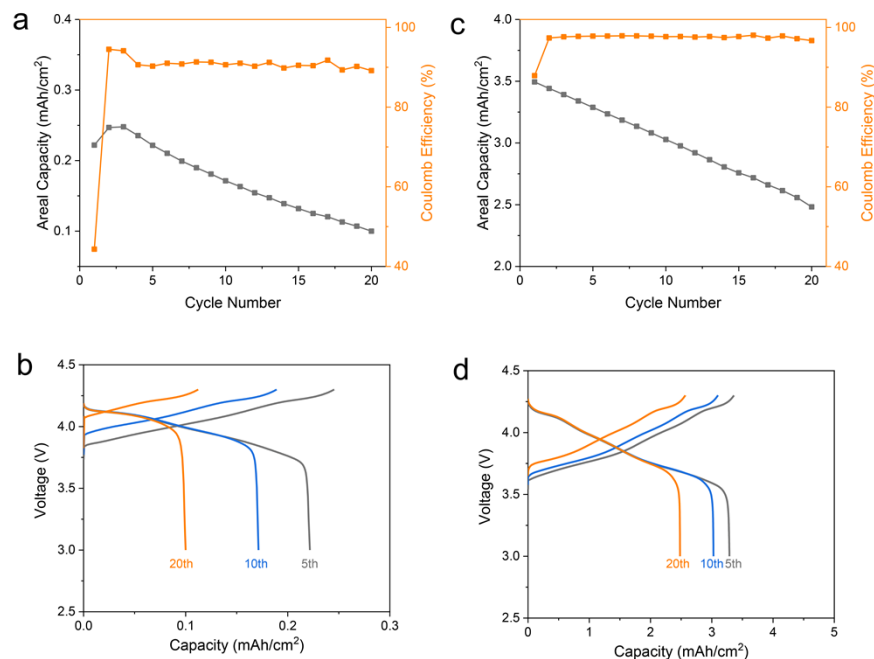


Figure S4 Electrochemical performance of Cu||NCM811 AFLMBs. Cycling performance with CEs of **a**, Cu||thin NCM811 and **c**, Cu||thick NCM811 batteries. The corresponding galvanostatic charge/discharge profiles of **b**, Cu||thin NCM811 and **d**, Cu||thick NCM811 batteries. The batteries were cycled at a current density of 0.5 mA/cm² and a voltage range of 3.0 and 4.3 V.

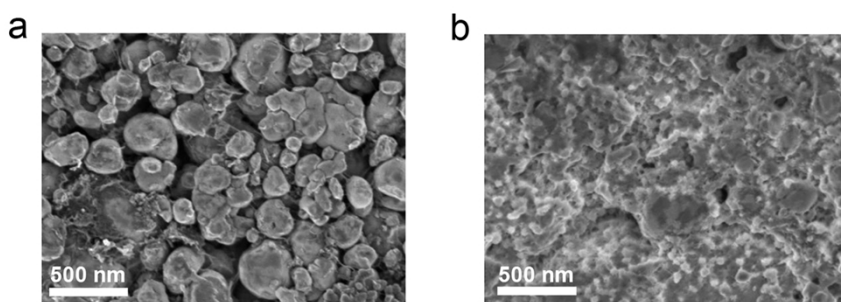


Figure S5 Morphological characterization of LFP cathode. **a**, SEM images of fresh LFP. **b**, SEM images of LFP after 150 cycles.

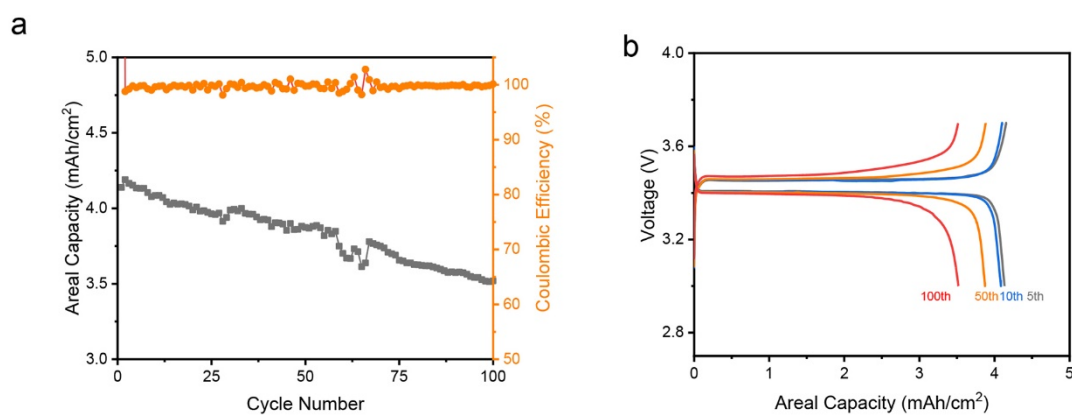


Figure S6 Electrochemical performance of Li||LFP batteries using cycled LFP in AFLMBs. a, Cycling performance with CEs. **b,** The corresponding galvanostatic charge/discharge profiles. The batteries were first cycled at a current density of 0.25 mA/cm² for the formation cycle, followed by charge/discharge a current density of 0.5 mA/cm². The LFP cathode was obtained from Cu||LFP batteries after 150 cycles.

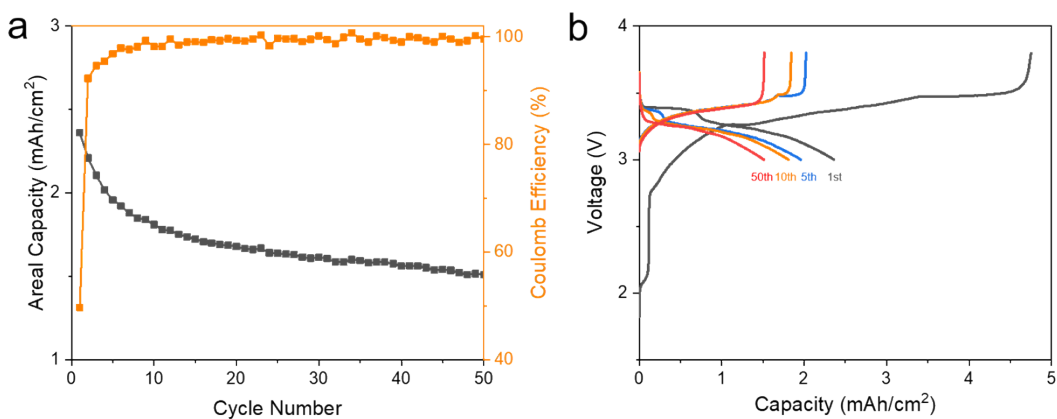


Figure S7 Electrochemical performance of CP||5LFP batteries. a, Cycling performance with CEs. **b,** The corresponding galvanostatic charge/discharge profiles. The batteries were cycled at a current density of 0.5 mA/cm^2 and a voltage range of 3.0 and 3.8 V.

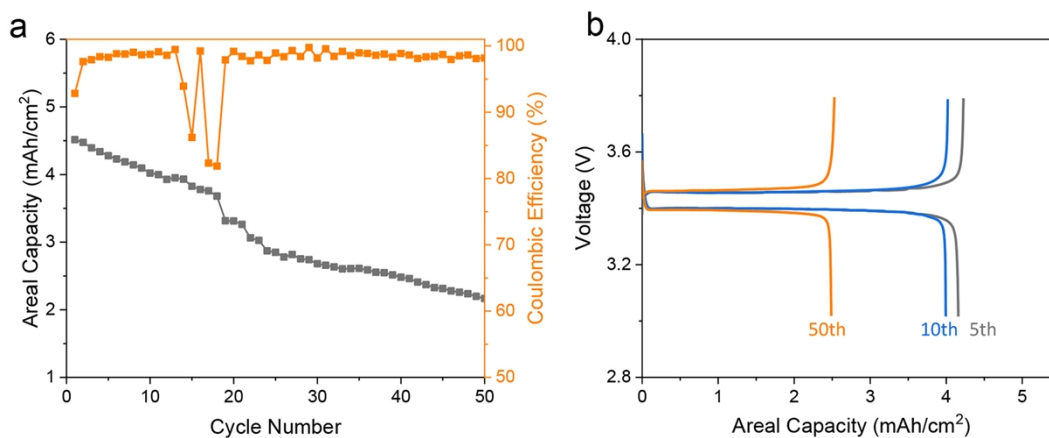


Figure S8 Electrochemical performance of Cu||5LFP batteries with lean electrolyte. a, Cycling performance with CEs **b,** The corresponding galvanostatic charge/discharge profiles. The usage of electrolyte was $15 \mu\text{L}$. The batteries were first cycled at a current density of 0.25 mA/cm^2 for the formation cycle, followed by charge/discharge a current density of 0.5 mA/cm^2 .

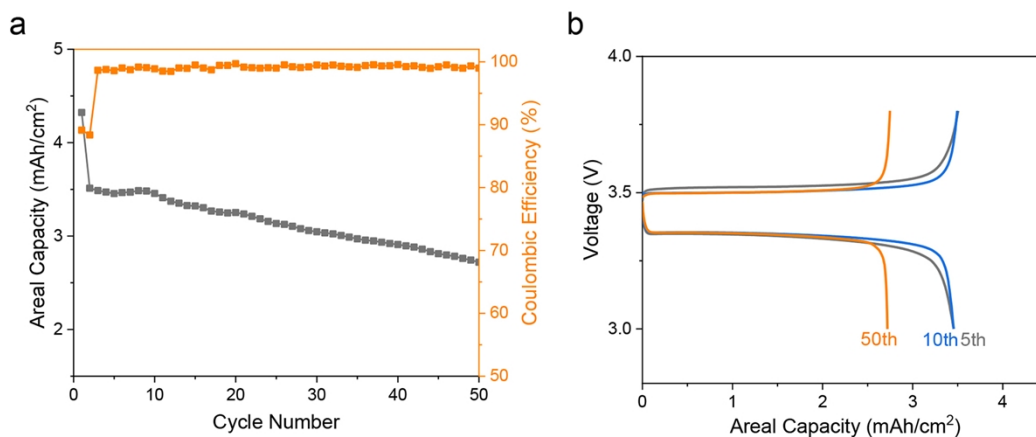


Figure S9 Electrochemical performance of Cu||5LFP batteries at 5 mA/cm². **a**, Cycling performance with CEs. **b**, The corresponding galvanostatic charge/discharge profiles. The batteries were first cycled at a current density of 0.25 mA/cm² for the formation cycle, followed by charge/discharge a current density of 5 mA/cm².

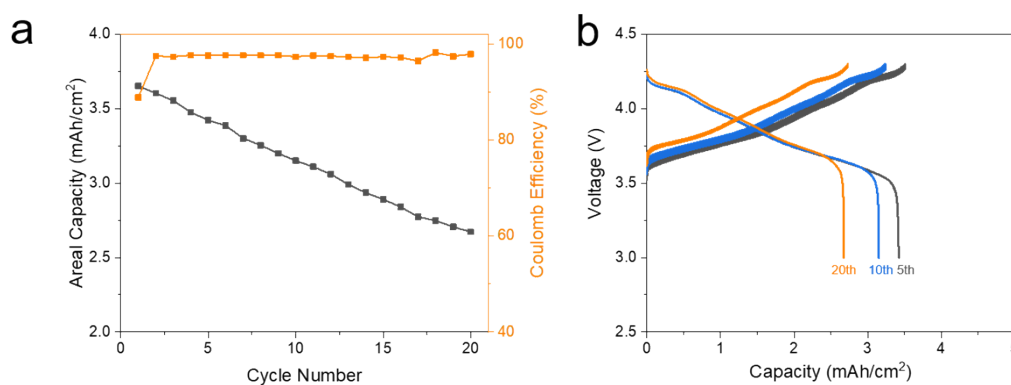


Figure S10 Electrochemical performance of Cu||NCM811 batteries with pc1,1 strategy. **a**, Cycling performance with CEs. **b**, The corresponding galvanostatic charge/discharge profiles.

Table S1 The relevant parameters used to calculate GED and VED in Fig 1 of the paper.

		Weight (mg/cm²)	Thickness (μm)
Cu foil/2		3.6	4
Li foil		2.7	50
Separator		1.1	20
Electrolyte		12	0
Al foil/2		2.2	8
Graphite	2.5 mAh/cm ²	7.0	46.7
LFP	0.5 mAh/cm ²	3.02	12.1
	2.5 mAh/cm ²	15.1	60.4
	5 mAh/cm ²	30.2	120.8
	10 mAh/cm ²	60.4	241.6

Table S2 A summary of reported AFLMB performance using LFP cathodes.

Strategy	Areal capacity	Current density	Capacity retention (50 cycle)	Details	Ref.
Anode Modification	~1.6 mAh/cm ²	0.5 mA/cm ²	56%	PI@Au	¹
	1.8 mAh/cm ²	0.1 C	66%	Mesoporous silica thin films (MSTFs) ⊥ SS	²
	0.675 mAh/cm ²	0.2 C	70.3%	Cu@PEO	³
	1.8 mAh/cm ²	0.1 C	78%	Multilayer Graphene	⁴
	~0.675 mAh/cm ²	Charge: 0.5 C Discharge: 1 C	51%	LiF@PVDF	⁵
	~2 mAh/cm ²	0.1 C / 0.4 C	89%	LiF-LiPON	⁶
	~2 mAh/cm ²	Formation: C/10, 3 cycles Regular cycling: C/3	59%	Ag@Cu	⁷
	0.74 mAh/cm ²	0.2 C	80%	PdTe ₂ @CuTe@Cu	⁸
Electrolyte Design	~1.5 mAh/cm ²	0.3 mA/cm ²	80%	tGPE PVDF-co-HFP, PHEMA	⁹
	1.6 mAh/cm ²	0.5 mA/cm ²	63%	3M LiFSI in DME/DOL (1:1, v/v)	¹⁰
	2 mAh/cm ²	1 mA/cm ²	73%	2 M LiFSI + 2 M LiNO ₃	¹¹
	1.6 mAh/cm ²	0.2 mA/cm ²	50%	2M LiFSI+1M LiTFSI in DME/DOL(1:1,v/v)	¹²
	~1.71 mAh/cm ²	Plate: 0.2 mA/cm ² Strip: 2.0 mA/cm ²	70%	4 M LiFSI-DME	¹³
Test Protocol	2 mAh/cm ²	Formation: C/10, 3 cycles Regular cycling: C/3	61%	Potential Hold	¹⁴
This work	~4.5 mAh/cm ²	0.5 mA/cm ²	79.4%	High loading + Pulse charge	
		5 mA/cm ²	78.0%		

References

1. H. H. Weldeyohannes, L. H. Abrha, Y. Nikodimos, K. N. Shitaw, T. M. Hagos, C.-J. Huang, C.-H. Wang, S.-H. Wu, W.-N. Su and B. J. Hwang, *J. Power Sources*, 2021, **506**, 230204.
2. C.-A. Lo, C.-C. Chang, Y.-W. Tsai, S.-K. Jiang, B. J. Hwang, C.-Y. Mou and H.-L. Wu, *ACS Appl. Energy Mater.*, 2021, **4**, 5132-5142.
3. A. A. Assegie, J.-H. Cheng, L.-M. Kuo, W.-N. Su and B.-J. Hwang, *Nanoscale*, 2018, **10**, 6125-6138.
4. A. A. Assegie, C. C. Chung, M. C. Tsai, W. N. Su, C. W. Chen and B. J. Hwang, *Nanoscale*, 2019, **11**, 2710-2720.
5. O. Tamwattana, H. Park, J. Kim, I. Hwang, G. Yoon, T.-h. Hwang, Y.-S. Kang, J. Park, N. Meethong and K. Kang, *ACS Energy Lett.*, 2021, **6**, 4416-4425.
6. J. Sun, S. Zhang, J. Li, B. Xie, J. Ma, S. Dong and G. Cui, *Adv. Mater.*, 2022, DOI: 10.1002/adma.202209404, e2209404.
7. W. Shin and A. Manthiram, *ACS Appl. Mater. Interfaces*, 2022, **14**, 17454-17460.
8. J. H. Lee, Y.-G. Cho, D. Gu and S. J. Kim, *ACS Appl. Mater. interfaces*, 2022, **14**, 15080-15089.
9. Y.-H. Lin, C.-Y. Shih, R. Subramani, Y.-L. Lee, J.-S. Jan, C.-C. Chiu and H. Teng, *J. Mater. Chem. A*, 2022, **10**, 4895-4905.
10. T. T. Beyene, B. A. Jote, Z. T. Wondimkun, B. W. Olbassa, C. J. Huang, B. Thirumalraj, C. H. Wang, W. N. Su, H. Dai and B. J. Hwang, *ACS Appl. Mater. Interfaces*, 2019, **11**, 31962-31971.
11. D. W. Kang, J. Moon, H.-Y. Choi, H.-C. Shin and B. G. Kim, *J. Power Sources*, 2021, **490**, 229504.
12. T. T. Beyene, H. K. Bezabh, M. A. Weret, T. M. Hagos, C.-J. Huang, C.-H. Wang, W.-N. Su, H. Dai and B.-J. Hwang, *J. Electrochem. Soc.*, 2019, **166**, A1501.
13. J. Qian, B. D. Adams, J. Zheng, W. Xu, W. A. Henderson, J. Wang, M. E. Bowden, S. Xu, J. Hu and J.-G. Zhang, *Adv. Funct. Mater.*, 2016, **26**, 7094-7102.
14. W. Shin and A. Manthiram, *Angew. Chem., Int. Ed.*, 2022, **61**, e202115909.